4. CO_2 condenses into the solid phase at a temperature of ~148 K at the average martian surface pressure of ~610 Pa.
5. H. H. Kieffer *et al.*, *Science* **194**, 1341 (1976).
6. H. H. Kieffer *et al.*, *J. Geophys. Res.* **84**, 8263 (1979).
7. D.A. Paige *et al.*, *J. Geophys. Res.* **95**, 1319 (1990).
8. Martian atmosphere consists of 95% of CO_2. Column abundance of water in the martian atmosphere is on the order of 10^{-3} g cm^{-2}, which is the equivalent of 10 precipitable μm. During northern summer the abundance increases to 100 μm above the cap (*35*).
9. S. W. Squyres, S. M. Clifford, R. O. Kuzmin, J. R. Zimbleman, F. M. Costard, in *Mars*, H. H. Kieffer, B. M. Jakosky, C. W. Snyder, M. S. Matthews, Eds. (Univ. of Ariz. Press, Tucson, 1992), pp. 523–554.
10. Ground ice is stable where it is in equilibrium with the water vapor content of the martian atmosphere (*36*).
11. M. H. Carr, *Water on Mars* (Oxford, New York, 1996).
12. S. M. Clifford, T. J. Parker, *Icarus* **154**, 40 (2001).
13. D. M. Drake, W. C. Feldman, B. M. Jakosky, *J. Geophys. Res.* **93**, 6353 (1988).
14. W. C. Feldman, W. V. Boynton, B. M. Jakosky, M. T. Mellon, *J. Geophys. Res.* **98**, 20855 (1993).
15. J. Masarik, R. J. Reedy, *J. Geophys. Res.* **101**, 18891 (1996).
16. W. V. Boynton *et al.*, *Space Sci. Rev.*, in press.
17. W. C. Feldman *et al.*, *Science* **297**, 75 (2002).
18. I. G. Mitrofanov *et al.*, *Science* **297**, 78 (2002).
19. W. V. Boynton *et al.*, *Science* **297**, 81 (2002).
20. It is typical to express seasonal changes on Mars with respect to solar longitude, L_s , which runs from 0° to 360°, with 0° corresponding to the vernal equinox in the northern hemisphere. Odyssey mapping stage started at 18 February 2002 (L_s = 330° before the recent vernal equinox at 18 April 2002). The HEND data are presented until 8 April 2003 (L_s = 165° after the recent equinox at 18 April 2002).
21. Epithermal neutrons have energies from 0.4 eV up to 1 MeV. These neutrons provide the most evident signature for the presence of subsurface water.
22. P. B. James, B. A. Cantor, *Icarus* **154**, 131 (2001).
23. H. H. Kieffer *et al.*, *J. Geophys. Res.* **105**, 9653 (2000).
24. M. T. Zuber *et al.*, *J. Geophys. Res.* **97**, 7781 (1992).
25. D. E. Smith *et al.*, *J. Geophys. Res.* **106**, 23689 (2001).
26. MOLA is a 10-Hz laser ranging system that measures the topography of Mars (*37*). Before averaging, topography measurements have an accuracy of <1 m, but with averaging the accuracy in latitudinal annuli can be improved to ~10 cm, which is suitable to detect seasonal changes in surface height produced by the condensation and sublimation of CO_2 (*27*). Time variations in topography from MOLA were measured during the period 28 February 1999 through 25 May 2001.
27. D. E. Smith, M. T. Zuber, G. A. Neumann, *Science* **294**, 2141 (2001).
28. Although interannual variations in seasonal snowfall may occur at least on a regional scale (*38*), the global trends would be expected to correspond to the level of detectability if CO_2 condensation and sublimation were primarily controlled by solar insolation (*3*).
29. All four layers may contribute to the layer of neutron production. Calculations of neutron emission from the layer of neutron production were performed by standard MCNPX code (*39*).
30. H. Wanke, J. Bruckner, G. Dreibus, R. Reider, I. Ryabchikov, *Space Sci. Rev.* **96**, 317 (2001).
31. Measurements from the Viking-1 lander indicated that the content of bound water in the upper layer is in the range 0.1 to 3% (*32*). Recent Mars Odyssey in-flight calibration models (GRS, HEND, and NS data) based on 100% of H_2O in north residual polar cap suggest that this value could be between 2 and 3 %. In our study we assumed 3 wt % H_2O in the uppermost dry layer of the subsurface, which leads to the most conservative estimate of water-ice content below it.
32. K. Biemann, *J. Mol. Evol.* **14**, 65 (1979).
33. Neutron fluxes have been normalized to unity for the maximum flux from the Solis Planum region, the driest region of Mars and an area not affected by seasonal CO_2 precipitation (Fig. 1; 270°E, 25°S). This normalization allows us to exclude the effect of temporal variations of neutron emission of Mars due to variable flux of charge particles from the Sun. To estimate absolute values of water content in different regions of Mars it is necessary to determine the amount of water in this reference region. Numerical calculations show that the best agreement between neutron measurements and a regolith model with a soil with Pathfinder composition (*30*) and free parameter of water content corresponds to 1.5 to 2 wt % H_2O. To establish a conservative lower-limit estimation for water content in other regions of Mars, we have accepted 1.5% for the reference value for the Solis Planum region.
34. For an average soil density of 1.6 g/cm^3, the column density of 10 g/cm^2 for 80° to 85°N corresponds to 6-cm thickness of upper drier layer, the column density of 40 g/cm^2 for 70° to 79°N corresponds to the linear thickness of 25 cm, and the column density of 60 g/cm^2 for 65° to 69°N implies 37 cm of drier soil above the water ice–rich ground.
35. B. M. Jakosky, C. B. Farmer, *J. Geophys. Res.* **87**, 2999 (1982).
36. C. B. Farmer, P. E. Doms, *J. Geophys. Res.* **84**, 2881 (1979).
37. D. E. Smith *et al.*, *Science* **284**, 1495 (1999).
38. M. C. Malin, K. S. Edgett. *J. Geophys. Res.* **106**, 23429 (2001).
39. L. S. Waters, Ed., MCNPX User's Guide (document LA-UR-99-6058, Los Alamos National Laboratory, Los Alamos, NM, 1999).
40. Because HEND has a wide field of view, the signal in each pixel represents the superposition of many nearby pixels. The horizontal resolution is about 300 km.

41. We acknowledge the Mars Odyssey and Mars Global Surveyor spacecraft and operation teams at the Jet Propulsion Laboratory and Lockheed-Martin Astronautics. The HEND and MOLA investigations are supported by NASA's Mars Exploration and Data Analysis Programs. M.T.Z. acknowledges support from a fellowship from the Radcliffe Institute for Advanced Study at Harvard.

10 March 2003; accepted 28 May 2003

Equatorially Dominated Magnetic Field Change at the Surface of Earth's Core

Christopher C. Finlay* and Andrew Jackson

Slow temporal variations in Earth's magnetic field originate in the liquid outer core. We analyzed the evolution of nonaxisymmetric magnetic flux at the core surface over the past 400 years. We found that the most robust feature is westward motion at 17 kilometers per year, in a belt concentrated around the equator beneath the Atlantic hemisphere. Surprisingly, this motion is dominated by a single wavenumber and persists throughout the observation period. This phenomenon could be produced by an equatorial jet of core fluid, by hydromagnetic wave propagation, or by a combination of both. Discrimination between these mechanisms would provide useful constraints on the dynamics of Earth's core.

A dynamo mechanism operates in Earth's liquid outer core: Convective motions induce electrical currents, which in turn produce the geomagnetic field (*1*). The details of this process are complex, and the generated field varies in time and space. Regularized inversion techniques (*2*), using observations made by mariners, magnetic observatories, magnetic surveys, and satellites, have been used to obtain images of the magnetic field at the core surface. A recent compilation of all suitable direct observations of the field has been used to construct a time-dependent field model (*3*), which is our most complete picture of the evolution of the magnetic field over the past 400 years. It is important that the information contained in this model be fully exploited and used to constrain and inform the development of rapidly improving models of the geodynamo (*4, 5*).

Here, we systematically decompose the radial magnetic field at the core surface, retaining only the nonaxisymmetric part, which varies on time scales shorter than the 400-year historical record; we refer to this as the residual field. Our method enables us to follow changes in the field morphology over the entire span of observations and does not rely on knowledge of the field strength, which was measured only after 1830. Nonaxisymmetric fields in the core are known to be important for maintaining the geodynamo (*6*), and their motions produce field changes observed at Earth's surface (*7–9*). Geodynamo models also display concentrations of nonaxisymmetric field (*10*)—for example, at points where fluid flow near the core surface converges—although the mechanism producing the motion of such flux foci remains poorly understood.

The radial magnetic field B_r at the core surface was sampled every 2° in latitude and longitude and every 2 years in time. We removed the time-averaged axisymmetric field and high-pass filtered in the time domain to remove that part of the signal containing periods longer than 400 years. The residual field is typically only 10% of the

School of Earth Sciences, University of Leeds, Leeds LS2 9JT, UK.

*To whom correspondence should be addressed. E-mail: c.finlay@earth.leeds.ac.uk

magnitude of the original signal B_r, but captures 42% of the change observed at the core surface (*11*). Consequently, we are able to isolate new aspects of the field evolution that were previously obscured. Rather than a static picture with small-amplitude features riding on top, the processed data of the residual field reveal a dynamic field morphology that evolves rapidly over the 400 years studied (Fig. 1) (movie S3). In the equatorial region we observe a series of high-amplitude flux foci moving westward. Field changes are most obvious under the Atlantic hemisphere while less activity occurs under the Pacific hemisphere, suggesting some longitudinal modulation of the field or of the mechanism causing its motion (*12, 13*).

We constructed time-longitude diagrams (*14–16*) of the residual field every 2° of latitude in order to view zonal motions, which are important in rapidly rotating fluids such as Earth's liquid outer core because of the influence of strong Coriolis forces. Westward motion of a succession of flux foci was observed at the equator (Fig. 2A) and less clearly at mid-latitudes (e.g., Fig. 2B at 40°S). Two-dimensional frequency-wavenumber power spectra were calculated from the time-longitude diagrams. Peaks in these spectra pinpoint the preferred zonal wavenumbers m (where $m = 360°/\lambda$ and λ is the angular wavelength in degrees) and frequencies f (where $f = 1/T$ and T is the period in years) of the zonal motion of the residual field at each latitude. At the equator, the dominant wavenumber was $m = 5$ (i.e., $\lambda = 72°$) and $f = 3.75 \times 10^{-3}$ year^{-1} (i.e., $T = 270$ years), whereas at 40°S, the field change was less monochromatic with more power at lower wavenumbers. At 20°N, we found a strong $m = 8$ signal consistent with high-resolution maps of the radial magnetic field at the core surface, recently obtained from satellite measurements (*17*).

The gradient of a diagonal line produced by a moving feature in a time-longitude diagram measures the apparent zonal speed of that feature. We determined the power traveling at all possible gradients in our time-longitude diagrams by means of a technique based on the Radon transform (*18, 19*). A prominent peak at the equator (Fig. 3) identifies the highest amplitude, most robust zonal motion of the residual field in the record, at a speed of 17 km year^{-1} (0.27° year^{-1}) westward. Less pronounced peaks were found at latitudes 55°N (18 km year^{-1} or 0.49° year^{-1}) and at 40°S (26 km year^{-1} or 0.56° year^{-1}). To assess the longevity of the peaks, we applied the Radon speed determination method to time subwindows of the time-longitude diagrams. We found that the striking equatorial peak was present throughout, whereas the smaller peak at 55°N was obvious only from 1750 to 1880 and the peak at 40°S was strongest from 1800 to the present.

Observations of zonal motion of magnetic field at low latitudes can be accounted for by two rather different mechanisms, both of which could conceivably be occurring at the surface of Earth's core. One possibility is that a westward equatorial jet

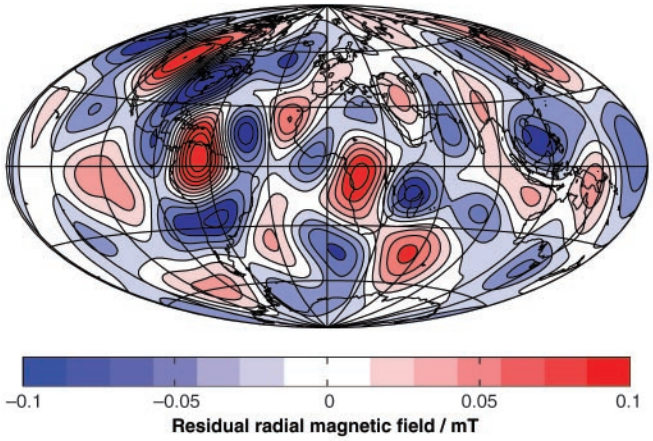

Fig. 1. Snapshot of the nonaxisymmetric radial magnetic field, high-pass filtered with a cut-off period of 400 years (referred to in the text as the residual field), shown at the core surface in 1850.

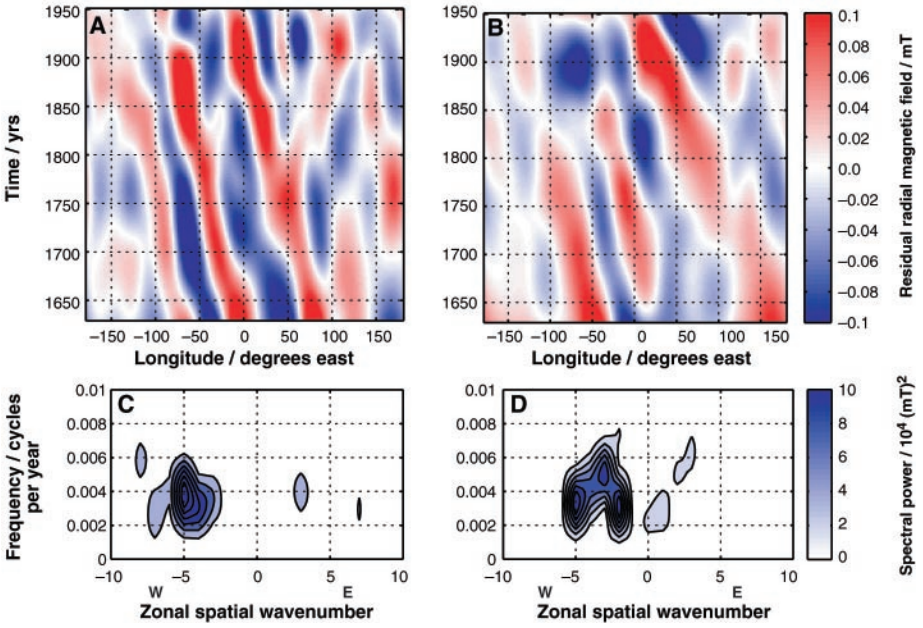

Fig. 2. Time-longitude diagrams of the residual field at specific latitudes (**A**) 0° (the equator) and (**B**) 40°S. Frequency-wavenumber spectra of these time-longitude diagrams are shown in (**C**) and (**D**), respectively; peaks pinpoint the dominant zonal wavenumbers (m) and frequencies ($f = 1/T$, where T is the period) of the zonal field motions.

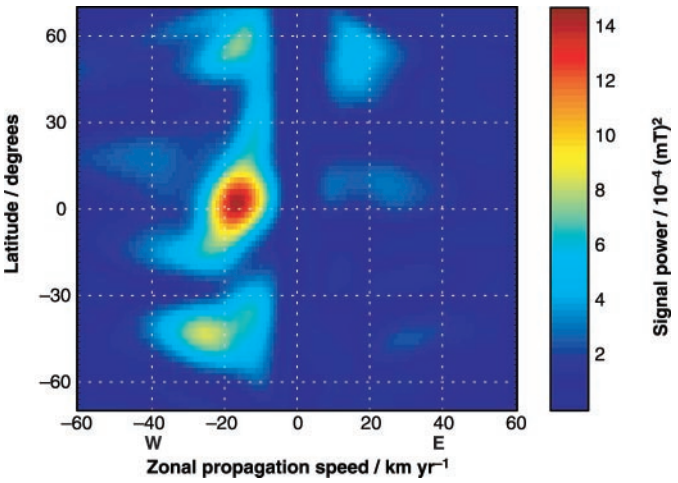

Fig. 3. Power moving with eastward zonal speeds between −60 and 60 km year^{-1} in time-longitude diagrams of the residual field, every 2° latitude from 70°N to 70°S. A maximum is found at the equator, indicating a robust measurement of westward motion (at −17 km year^{-1}) in this region. Weaker signals are observed at mid-latitudes, particularly near 40°S (−26 km year^{-1}) and 55°N (−18 km year^{-1}).

could be bodily transporting core fluid, and thus magnetic field lines (that move with the fluid to a first approximation), from east to west. Such an equatorial jet has previously been suggested in inversions of radial magnetic field change for core flows (*20*), and strong westward (retrograde) zonal flows produced by nonlinear Reynolds stresses have been observed in rotating convection experiments (*21*). Another mechanism that could play a role is an equatorially confined MAC (magnetic, Archimedes, Coriolis) wave (*22, 23*), driven by either convective (*24*) or magnetic (*25*) instability. This phenomenon would produce a series of propagating upwellings and downwellings at the core surface, with motion of associated flux foci. Because equatorial MAC waves would have propagation properties dependent on the strength of the core's hidden toroidal magnetic field, it may be possible to use these waves to estimate this parameter, which defines the nature of the dynamo process. Successful quantification of the relative contributions of these two mechanisms would be a valuable constraint on models of the geodynamo.

References and Notes

1. P. H. Roberts, G. A. Glatzmaier, *Rev. Mod. Phys.* **72**, 1081 (2000).
2. D. Gubbins, J. Bloxham, *Geophys. J. R. Astron. Soc.* **80**, 695 (1985).
3. A. Jackson, A. R. T. Jonkers, M. R. Walker, *Philos. Trans. R. Soc. London Ser. A* **358**, 957 (2000).
4. E. Dormy, J.-P. Valet, V. Courtillot, *Geochem. Geophys. Geosyst.* **1**, 2000GC000062 (2000).
5. M. Kono, P. H. Roberts, *Rev. Geophys.* **40**, 2000RG00102 (2002).
6. S. I. Braginsky, *Sov. Phys. JETP* **47**, 1084 (1964) [English translation: *Sov. Phys. JETP* **20**, 726 (1965)].
7. E. C. Bullard, C. Freedman, H. Gellman, J. Nixon, *Philos. Trans. R. Soc. London Ser. A* **243**, 67 (1950).
8. R. Hide, *Philos. Trans. R. Soc. London Ser. A* **259**, 615 (1966).
9. J. Bloxham, D. Gubbins, A. Jackson, *Philos. Trans. R. Soc. London Ser. A* **329**, 415 (1989).
10. P. Olson, U. Christensen, G. A. Glatzmaier, *J. Geophys. Res.* **104**, 10383 (1999).
11. For further details on the processing methods, see supplementary material at *Science* Online.
12. It has long been recognized that smaller changes in the magnetic field occur under the Pacific hemisphere than under the Atlantic hemisphere, possibly because of the influence of the deep mantle on core motions (*13*). Here we found that between 1630 and 1950, 50% more RMS variation in the residual field occurred under the Atlantic hemisphere than under the Pacific hemisphere. In movie S3 we observe that the strong equatorial flux foci do not travel into the Pacific hemisphere, hence the mechanism causing the westward motion of flux foci is disrupted under Central America.
13. R. Hide, *Science* **157**, 55 (1967).
14. E. Hövmoller, *Tellus* **1**, 62 (1949).
15. B. C. Chelton, M. G. Schlax, *Science* **272**, 234 (1996).
16. M. Wheeler, G. N. Kiladis, *J. Atmos. Sci.* **56**, 374 (1999).
17. A. Jackson, in preparation.
18. K. L. Hill, I. S. Robinson, P. Cipollini, *J. Geophys. Res.* **105**, 21927 (2000).
19. S. R. Jeans, *The Radon Transform and Some of Its Applications* (Wiley, New York, 1988).
20. J. Bloxham, *Geophys. J. Int.* **99**, 173 (1989).
21. J. Aubert, D. Brito, H.-C. Nataf, P. Cardin, J.-P. Masson, *Phys. Earth Planet. Inter.* **128**, 51 (2001).
22. S. I. Braginsky, *Geomagn. Aeron.* **7**, 851 (1967).
23. P. H. Roberts, A. Soward, *Annu. Rev. Fluid Mech.* **4**, 117 (1972).
24. K. Zhang, D. Gubbins, *Math. Comp. Model.* **36**, 389 (2002).
25. K. Zhang, D. R. Fearn, *Geophys. Astrophys. Fluid Dyn.* **77**, 133 (1994).

26. We thank D. Gubbins and R. Hide for helpful discussions. Supported by UK Natural Environment Research Council Studentship NER/S/A/2001/06265 (C.C.F.).

Supporting Online Material

www.sciencemag.org/cgi/content/full/300/5628/2084/DC1
Materials and Methods
Figs S1 to S6
Movies S1 to S3

11 February 2003; accepted 28 May 2003

Changes in Ocean Water Mass Properties: Oscillations or Trends?

Harry L. Bryden,* Elaine L. McDonagh, Brian A. King

A new transindian hydrographic section across 32°S reveals that thermocline mode waters have become saltier and colder since 1987. This change almost entirely reverses the observed freshening of mode waters from the 1960s to 1987 that has been interpreted to be the result of anthropogenic climate change on the basis of coupled climate models. Here, we compare five hydrographic sections from 1936, 1965, 1987, 1995, and 2002 to show that upper thermocline waters (10°C to 17°C) changed little from 1936 to 1965, freshened from 1965 to 1987, and since 1987 have become saltier. These results demonstrate substantial oscillations in mode-water properties.

When so few oceanographic sections have been sampled more than once, it is notable that the remote Indian Ocean section across 32°S has now been completely occupied four times. The first transindian section in 1936 was made as part of the Royal Research Ship (RRS) *Discovery* expeditions (*1*). The second aboard Research Vessel (R/V) *Atlantis II* in 1965 was part of the Indian Ocean Expedition (*2*). The third in 1987 was fitted into RRS *Charles Darwin*'s inaugural round-the-world voyage (*3*). The World Ocean Circulation Experiment (WOCE) managed only to reoccupy the eastern and western parts of the section aboard R/V *Knorr* in 1995 (*4*, *5*). In March and April of 2002, we reoccupied the 32°S transindian section aboard *Darwin* with a principal goal to measure the meridional overturning circulation across this southern boundary of the Indian Ocean. In view of the previous sections and because of interest in the use of changes in thermocline mode-water properties as a "fingerprint" for anthropogenic climate changes (*6*–*9*), our first effort was to examine the evolution of water mass properties from 1936 to the present.

Our station track for the 2002 section followed the 1987 section from the coast of South Africa out to 80°E (Fig. 1), after which we deviated from the 1987 track in order to improve the estimation of the overturning circulation. For this reason, we initially made comparisons between the 1987 and 2002 measurements west of 80°E where the sections coincide. Taking advantage of the tight potential temperature–salinity (θ-S) relationship, which is not affected by the mesoscale eddy variability evident in the large vertical excursions of water masses from station to station, we found the salinity on potential temperature surfaces (*10*) at each station and then examined the salinity difference (between 1987 and 2002) on isotherms along the section (Fig. 2). The changes are remarkably uniform along the section: Upper thermocline waters between 10°C and 17°C are saltier by as much as 0.06, whereas lower thermocline waters between 5°C and 10°C are fresher by as much as 0.03.

It is common to estimate changes in ocean properties on isopycnal surfaces (*11*–*14*). We found that the change in zonally averaged salinity on isopycnal surfaces achieves a maximum of 0.09 at a neutral density of 26.66 (at a temperature of about 12.9°C). Such an increase in salinity is opposite to the freshening from the 1960s to 1987, which achieved a maximum of –0.12 at a neutral density of 26.75 (*13*). As a result of becoming fresher from the 1960s to 1987 and becoming saltier from 1987 to 2002, the upper thermocline waters now have nearly the same properties they had in the 1960s.

Because the shape of the θ-S relationship lies somewhat parallel to the isopycnals (fig. S1A), changes on isopycnal surfaces can exaggerate trends. We prefer to report the minimum change in water mass

Southampton Oceanography Centre, Empress Dock, Southampton SO14 3ZH, UK.

*To whom correspondence should be addressed. E-mail: h.bryden@soc.soton.ac.uk